Nuclear Engineering and Technology 51 (2019) 776–783

Contents lists available at ScienceDirect

Nuclear Engineering and Technology

journal homepage: www.elsevier.com/locate/net

Original Article

Pulsed laser welding of Zr–1%Nb alloy

Maxim A. Elkin, Alexey S. Kiselev, Mikhail S. Slobodyan*

Tomsk Polytechnic University, Russia

ARTICLE INFO

Article history:
Received 16 July 2018
Received in revised form
3 December 2018
Accepted 21 December 2018
Available online 24 December 2018

Keywords:
Zirconium alloys
Pulsed laser welding
Butt welds
Mechanical properties
Microstructure
Defects

ABSTRACT

Laser welding is usually a more effective method than electron-beam one since a vacuum chamber is not required. It is important for joining Zr–1%Nb (E110) alloy in a manufacturing process of nuclear fuel rods. In the present work, effect of energy parameters of pulsed laser welding on properties of butt joints of sheets with a thickness of 0.5 mm is investigated. The most efficient combination has been found (8–11 J pulse energy, 10–14 ms pulse duration, 780–810 W peak pulse power, 3 Hz pulse frequency, 1.12 mm/s welding speed). The results show that ultimate strength under static loading can not be used as a quality criterion for zirconium alloys welds. Increased shielding gas flow rate does not allow to protect weld metal totally and contributes to defect formation without using special nozzles. Several types of imperfections of the welds have been found, but the major problem is branching microcracks on the surface of the welds. It is difficult to identify the cause of their appearance without additional research on improving the welding zone protection (gas composition and flow rate as well as nozzle configuration) and studying the hydrogen content in the welds.

1. Introduction

Enhancing safety, extending burnup, reducing maintenance and fuel cycle costs are the main directions of development of the nuclear industry [1]. Zirconium alloys are used as a structural material for nuclear fuel assemble production of water cooled reactors (VVER, PWR, CANDU, BWR and RBMK). They are classified according to basic alloying elements: tin (Zircaloy-2 and Zircaloy-4), niobium (E110, E125, M5, Zr-2.5%Nb) and multi-element (E635, ZIRLO, NDA, MDA, etc.) [2]. The specificity of zirconium alloys is strong influence of impurities in the metal on its performance properties [3]. Due to this fact, the maximum concentration of impurities in Zr–Nb alloys is regulated by the standard [4], but, for instance, the content of widely used E110 alloy (Zr–1%Nb) is much lower in most cases [5]. Rolled metal of E110 alloy is supplied in recrystallised annealing condition. It has microstructure, which includes α-Zr matrix with Nb precipitations (grain size of 3–4 μm) and β-Nb with size 40–60 nm. Presence of β-Zr as well as metastable α′–Zr and ω-Zr is undesirable, because it significantly decreases corrosion resistance and deteriorates another characteristics [5]. It should be noted that the values of tensile strength of the Zr–Nb alloys used for nuclear fuel assemble production are unstable due to non-isotropic nature of the metal. This parameter also depends even on minor changes in chemical and phase composition, microstructure and texture. The allowable range of tensile strength at room temperature is considered to be 400–800 MPa [5,6].

One of the most important operations in the technology of manufacturing fuel assembles is welding. It significantly changes structure and properties of metal. End parts are joined to fuel rods by electron-beam and resistance butt welding, while parts of spacing grids are joined to each other by resistance spot and laser welding [2]. Requirements for welders, welding materials, equipment and technologies as well as quality of welded joints are regulated by standards [7–11]. Despite their existence, the problem of fuel rods failure during operation, including that due to factory defects of welds, has been very important until now [12,13]. For this reason, many researchers work on optimization of the conventional welding technologies and development of new methods [14]. For example, laser welding may be a more effective method than electron-beam one for joining E110 alloy in the manufacturing process of nuclear fuel rods for VVER. A vacuum chamber is not required for laser welding, thus it increases the efficiency of the process and reduces burn-out of alloying elements.

The processes of laser welding of various metals and alloys have been studied for half a century [15,16]. However, development of a welding technology for each new combination of the type and the dimensions of joints as well as material compositions is still a

* Corresponding author. 30, Lenin avenue, Tomsk, 634050, Russia.
E-mail address: s.m.s@ngs.ru (M.S. Slobodyan).

https://doi.org/10.1016/j.net.2018.12.016

difficult task. It is obligatory to study the effect of welding parameters on the properties of the joints on the basis of general recommendations [15–18] and, if available, results of previously published data on close combinations. In addition, any methods of statistical data analysis can be applied.

Laser welding processes are classified into two main types depending on the ratio of energy input to a volume of melted metals. The first type, a conduction mode, is typical for welding thick-walled structures. A weld pool is formed due to dissipation of energy of a laser beam deep into the metals by thermal conductivity. The temperature of the weld pool is in the range between the melting and vaporization temperatures of the metals. Welds usually have a semicircular cross-section with a small aspect ratio. The second type, a keyhole mode, is used for welding relatively small work-pieces. This type of welding processes uses high values of heat input, and temperatures on surface of weld pools can exceed the boiling point.

Besides this, laser welding processes are divided into continuous and pulsed modes. In the case of continuous energy input, the main technological parameters are beam diameter focused at a surface d, welding speed V and laser power P. For pulsed modes, the determining energy parameters are pulse energy E, pulse duration τ, frequency f, and peak power P_{peak}:

$$P_{peak} = \frac{E}{\tau}. \quad (1)$$

Average power P_{ave} is calculated taking into account time duration between pulses τ_{off}:

$$P_{ave} = \frac{E}{\tau + \tau_{off}}. \quad (2)$$

Pulse frequency should be set taking into account the features of pulsed laser welds. When a welding process starts, the work-pieces are melted at one point during the first pulse. Then, the place where the laser beam interacts with the surface is shifted due to movement of the work-pieces or the welding head. The next pulse leads to melting of another metal volume, while a considerable part of energy is expended on heating of a part of the previously welded metal again. Overlapping factor of adjacent points OL is an important criterion affecting quality of the welds. It is determined by welding speed V, beam diameter d and frequency f by the following relationship:

$$OL = \frac{d - V/f}{d} \cdot 100\%. \quad (3)$$

Recommended values of OL are presented in Table 1. It should be noted that the results of multiple impact of thermal cycles on metal when welding two- or multi-phase materials can adversely affect their structure, formation of imperfections, high residual stresses and strains [19]. For this reason, the optimal value of OL should be determined taking into account structural and phase changes in the welded metal and heat affected zone during numerous thermal cycles.

All the above parameters are interdependent. Their values are determined by the thickness of the welded work-pieces, the configuration of the joint, thermo-physical and optical properties of the materials.

Table 1
Recommended overlapping factors (OL).

OL for typical non-hermetic welds, %	OL for hermetic welds, %	Reference
30–50	50–90	[15]
50–60	70–80	[16]
50–70	75–80	[17]
–	~70	[18]

Laser welding of zirconium alloys has been studied for many years. The first results of laser welding of Zircaloys [20,21], obtained more than three decades ago, have not been widely used. The main reasons were porosity and low corrosion resistance of the welds [22]. Furthermore, at that date laser welding equipment was unstable, had low efficiency and high cost [15,22]. Nevertheless, its constant improvement [16] has caused a significant amount of research in this field [23–45]. Most of them are devoted to welding of Zircaloys [23–38], including dissimilar joints with tantalum [39] and SiC/SiC composite [40]. Moreover, features of laser welding of commercially pure zirconium are considered in paper [41]. There is very few information on laser welding of other zirconium alloys, although it is known that all properties of similar welds may be radically different depending on the chemical composition of the alloys [46]. The exception is the papers devoted to welding of Zr-2.5%Nb alloy [42] and Zr-2.5Nb alloy to AISI 410 stainless steel with Ni filler [43]. In addition, recent papers [44,45] show the results of computer simulation of pulsed laser welding of E110 alloy. However, no experimental data on influence of welding parameters on properties of E110 welds has been found while preparing this article. Considering that the thickness of parts of nuclear fuel assembles does not exceed 1 mm in most cases, the most rational technology of their joining is keyhole pulsed laser welding [15–18]. In connection with information listed above, the aim of the paper is to determine effect of energy parameters of laser welding mode on weld width, structure, mechanical properties and presence of defects in butt-welded joints of sheets made of E110 alloy with a thickness of 0.5 mm.

2. Material and methods

Butt welded joints of two identical plates of E110 alloy with a thickness of 0.5 mm were investigated (specimens to be tested for tensile strength were 240 × 50 mm, samples for metallographic and microhardness tests were 100 × 24 mm). Chemical composition of E110 alloy is presented in Table 2. The edges of the work-pieces were machined for good fit-up using a miller and, just before welding, carefully degreased with acetone.

The work-pieces were welded without filler metal using a LTA-4-2 laser welding machine. Its technical characteristics are presented in Table 3. The angle between the laser beam and the work-pieces was 90°. The diameter of the focused beam d was 0.95 mm. The welding zone was protected from atmosphere on both sides using nozzles with a diameter of 10 mm (Fig. 1). Argon was used with a purity of >99.993%. The gas flow rate was 60 l/min similarly to papers [31,34,35], although the usual recommended ranges of values are much smaller: from 15 to 18 l/min [15] to 30–45 l/min [17].

Initially, the welding parameters were experimentally determined with no imperfections found during visual inspection of the welds (Table 4, mode 2). Then, nine more experimental modes were justified, taking into account the possibility of adjusting the laser facility. Three combinations of the parameters were used, all other conditions being equal (Table 4):

1. Welding speed V as well as pulse energy E were varied by adjusting the current I in the pump lamps (pulse duration τ and frequency f were constant) to determine the possibility of improving efficiency due to increase in the volume of the welded metal during one pulse (modes 1, 2, 3, 4).
2. Pulse durations τ were varied to determine the effect of the period of action of laser radiation on the metal on the properties

Table 2
Chemical composition of E110 alloy.

Element	Composition, ppm (wt, %)		Element	Composition, ppm (wt, %)	
	Max [4]	Typical [5]		Max [4]	Typical [5]
Zr	Balance	Balance	Cu	50	<10
Nb	0.9–1.1% (wt, %)	0.95–1.10% (wt, %)	Ti	50	<30
O	1000	500–700	Pb	50	<50
Hf	500	300–400	Mo	50	<30
Fe	500	140	K	40	<30
Sn	500	<100	Be	30	<30
Ca	300	<100	F	30	<30
Si	200	46–90	Cr	30	<7
Ni	200	30–39	Mn	20	<3
Cr	200	<30	H	15	4–7
C	200	40–70	B	5	<0.4
Al	80	<30	Cd	3	<0.3
N	60	30–40	Li	2	<2

Table 3
Parameters of the LTA-4-2 Nd:YAG pulsed laser facility.

Wave length, μm	1.064
Focal length, mm	100
Focal spot diameter, mm	0.2–2.0
Pulse frequency, Hz	1–150
Pulse duration, ms	2–20
Pulse energy, J	up to 50
Average power, W	up to 300
Welding speed, mm/s	up to 20

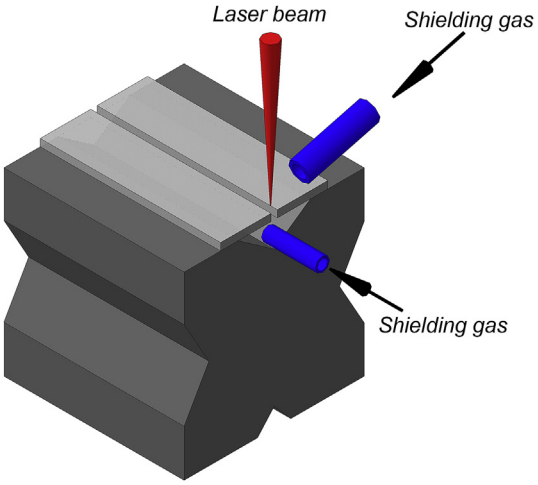

Fig. 1. Scheme of shielding gas blowing.

of the welded joints. Pulse energy E also changed because of the laser facility features, despite the same values of the current I in the pump lamps. Welding speed V and frequency f were the same (modes 5, 6, 2, 7).

3. Pulse frequency f was changed at the constant welding speed V to determine the most efficient overlapping factor OL. Pulse energy was unchanged due to the constant values of current I in the pump lamps and pulse duration τ (modes 2, 8, 9, 10).

The samples for metallography were prepared using standard methods of grinding and subsequent polishing. Solution of H_2O (20 ml), 20% NH_4F (30 ml) and HNO_3 (50 ml) was used for etching. Surfaces of welded joints and microstructure of cross-sections were studied using Olympus SZ-61 and Olympus GX-51 optical microscopes. A JEOL JSM-6000PLUS scanning electron microscope was used to study microstructure of cross-sections and fractography of surfaces after failure during mechanical tests, as well as energy dispersive X-ray spectroscopy (EDS analysis). The specimens for mechanical test were cut out using a milling machine in accordance with the requirements of the standard [47] (Fig. 2 and Table 5). Mechanical test was performed on a MIRI-100 K facility, loading rate was 1 mm/min. Microhardness was determined using a HVS-1000 microhardness tester according to the requirements of the standards [48,49]. Distance between prints was 100 μm, load was 100 g, holding time was 10 s.

Table 4
Welding parameters.

Mode number	I, A	τ, ms	E, J	V, mm/s	f, Hz	P_{peak}, W	P_{ave}, W	OL, %
1	90	14	8.68	0.88	3	620	26	69
2	100		10.88	1.12		780	32	61
3	110		12.86	1.35		920	38	53
4	120		14.95	1.49		1070	44	48
5	100	10	8.12	1.12		810	24	61
6		12	9.50			790	28	61
7		16	12.26			770	36	61
8		14	10.88		5	780	54	76
9			10.88		7	780	76	83
10			10.88		9	780	97	87

3. Results and discussion

The dependences of weld width as well as tensile strength of the joints on welding parameters are shown in Fig. 3. They coincide qualitatively with the fundamentals [15–18]. In the range of values

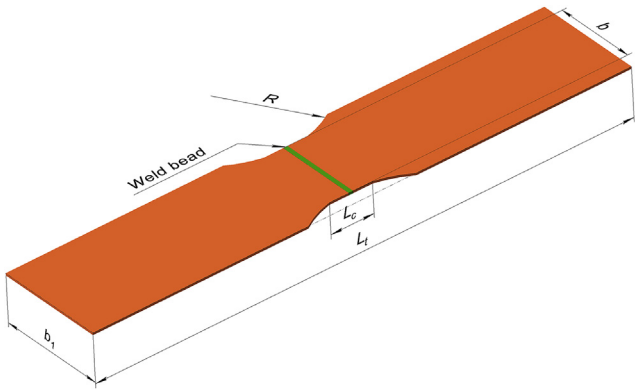

Fig. 2. Scheme of tensile test specimens [47].

Table 5
Dimensions of the tensile strength specimens [47].

Definition	Symbol	Dimension, mm
Overall length	L_t	240
Specimen width	b_1	50
Width of reduced section	b	38
Length of reduced section	L_c	25
Radius of fillet	R	25

studied, simultaneous increase in pulse energy and welding speed leads to linear increase in weld width and uniformity of depth penetration (Fig. 3, a). Simultaneous increase in pulse duration and its energy does not affect welds width on the upper side, but uniformity of penetration decreases due to heat losses to the base metal by thermal conductivity (Fig. 3, b). Increase in pulse frequency also does not affect weld width from the upper side, but the uniformity of depth penetration increases due to higher residual temperature between pulses (Fig. 3, c). It should be noted that there is no relationship between welding parameters and tensile strength of the joints in all cases studied. Five specimens failed along the base metal (modes 5, 6, 7, 8 and 9; Fig. 4, a), and other five through the welds: along the weld axis for modes 1 and 2 (Fig. 4, b), as well as through the weld and the base metal for modes 3, 4 and 10 (Fig. 4, c). The values of tensile strength for specimens failed through the beads (486–520 MPa) are slightly larger than for specimens failed through the base metal (455–496 MPa), but all of these are within the allowable range [5,6] and deviations from the average value (483 MPa) do not exceed 8%. Most probably, by analogy with titanium alloys [16], this is caused by the saturation of the metal with gases from the atmosphere. Double-sided protection of the welding zone and increased flow rates of high purity argon did not prevent contamination of the metal. This hypothesis is confirmed by dark discoloration along the welds (Fig. 4, c) and the results of EDS analysis of the welded metal after failure during the tensile test (Table 6, Fig. 5). Oxygen content is up to 61.5% by mass, and nitrogen is up to 8.81% by mass.

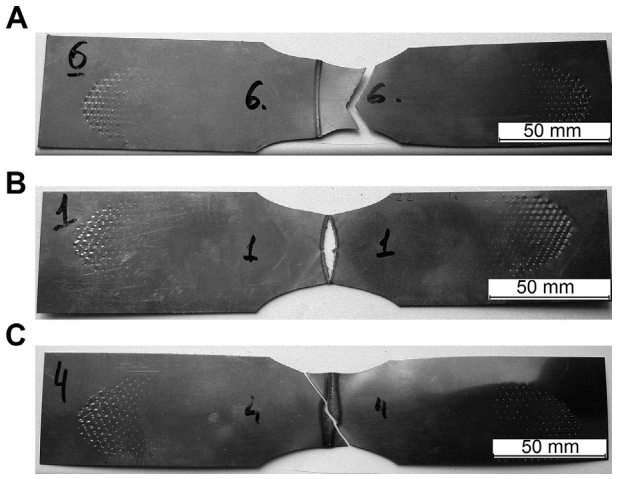

Fig. 4. Types of welded joints failure: a – through the base metal (mode 6), b – along the axis of the weld (mode 1), c – through the weld and the base metal (mode 4).

Table 6
Chemical composition of the welded metal after failure during the tensile test according to the results of EDS analysis.

Mode	Element (mass, %/atom, %)			
	Zr	Nb	O	N
1	31.65/7.51	0.98/7.51	61.50/83.21	5.86/9.05
2	82.83/46.32	1.10/0.60	12.01/38.31	4.06/14.77
3	75.06/34.72	1.08/0.49	18.84/49.69	5.01/15.10
4	63.83/23.60	1.44/0.52	25.92/54.65	8.81/21.23
10	88.05/56.98	0.75/0.48	8.87/32.74	2.33/9.80

Information on the presence of imperfections in the welded joints according to ISO 6520-1 [50] is summarized in Table 7,

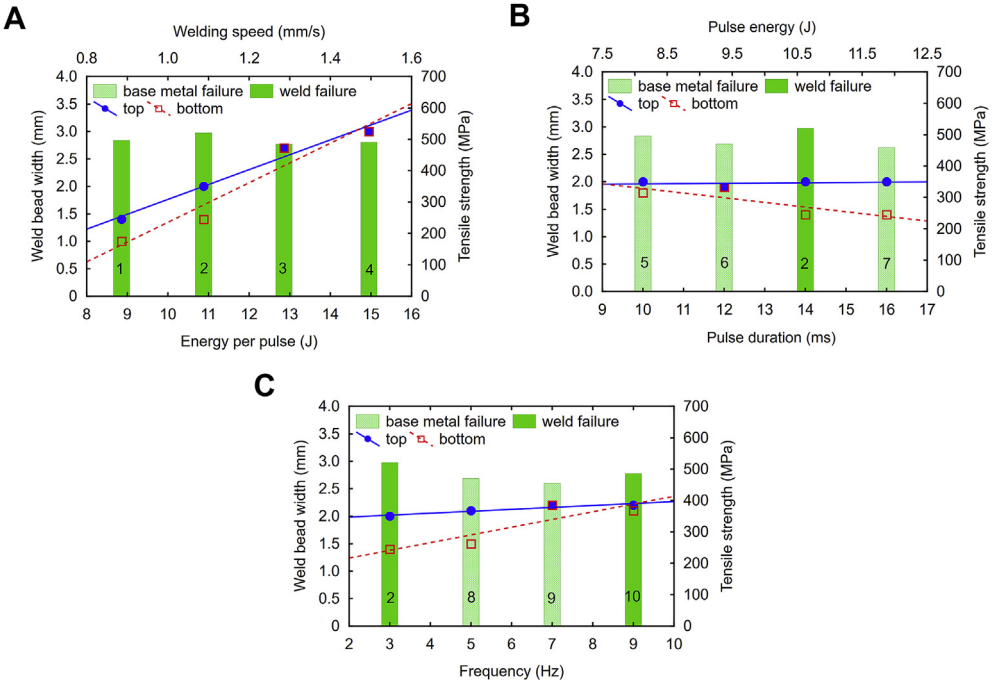

Fig. 3. Dependence of weld width and tensile strength of joints on welding parameters: a – pulse energy and welding speed (τ = 14 ms, f = 3 Hz; modes 1, 2, 3, 4), b – pulse duration and its energy (V = 1.12 mm/s, f = 3 Hz; modes 5, 6, 2, 7), c – frequency (E = 10.88 mm/s, τ = 14 ms, V = 1.12 mm/s; modes 2, 8, 9, 10).

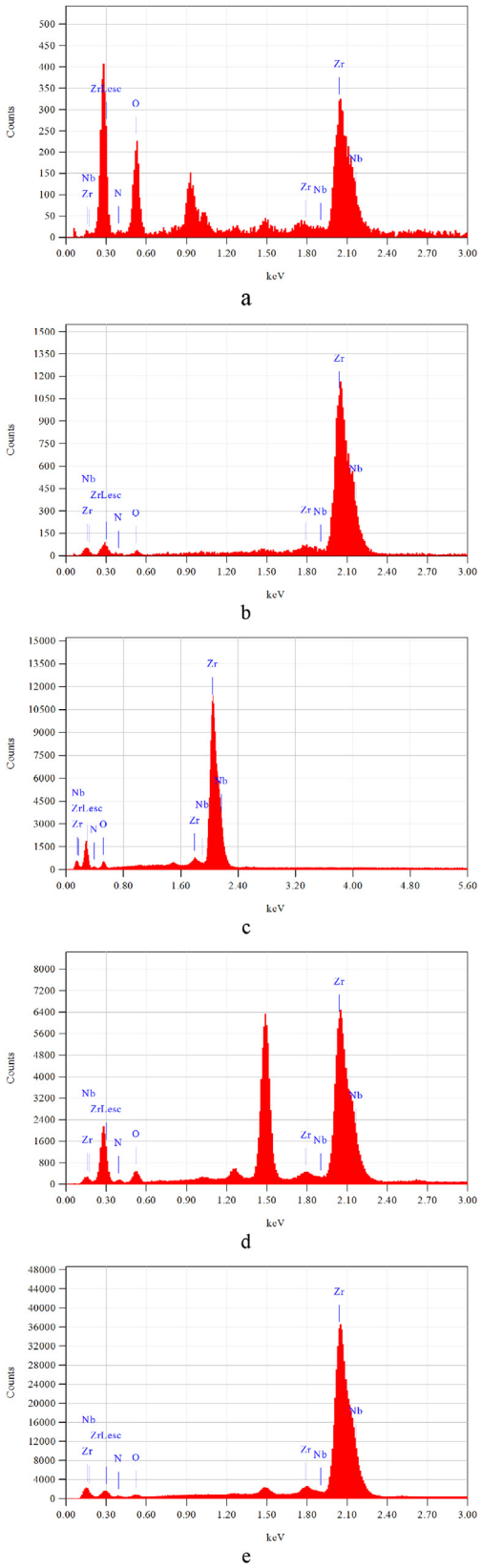

Fig. 5. Results of EDS analysis of the weld metal: a – mode 1, b –mode 2, c – mode 3, d – mode 4, e – mode 10.

Table 7
Imperfections in welded joints.

Type of imperfections	Welding mode									
	1	2	3	4	5	6	7	8	9	10
Discoloration			X	X			X	X	X	X
Spatter (bottom surface)			X	X						
Local intermittent undercuts								X		
Gas pores and cavities								X		
Longitudinal microcracks	X									X
Branching microcracks	X	X	X	X	X	X	X	X	X	X

Single pores with a diameter of less than 0.2 mm were not attributed to imperfections, since they do not significantly affect properties of welds [18].

examples are shown in Fig. 6. Some imperfections were identified for elevated values of heat input (modes 3, 4, 7, 8, 9 and 10). For high values of pulse energy (modes 3 and 4), spatter on bottom surface was observed in addition to contamination with gases (Fig. 6, a). Local intermittent undercuts, gas pores and cavities were also detected on the cross-section of the weld made using mode 8, (Fig. 6, b). The most likely cause of this fact was poor fit-up and increased shielding gas flow rate during welding [16–18].

The main problem of pulsed laser welding of E110 alloy according to the proposed technology was the presence of microcracks, which can be visible only using microscopes. Longitudinal microcracks along the edges of the weld (mode 1, Fig. 6, c) and in the center of the weld (mode 10, Fig. 6, d) were detected. The main cause of cracking along both sides of the weld using mode 1 is a small volume of the molten metal because of extremely low pulse energy. The features of laser welding are very high cooling rate of the metal and a narrow zone where plastic deformation is possible. When the amount of input energy is less than the optimum range of values, cooling rate exceeds the allowable limit and a brittle quenching martensitic structure with extremely high residual stresses is formed. For E110 alloy, this is the α' phase, which has an acicular structure (Fig. 7, a) and high microhardness (Fig. 8, a) [5,6,15,46]. Increasing the amount of input energy (modes 2, 5 and 6) makes it possible to form the weld metal structure with much smaller amount of martensite (Fig. 7b and c) and microhardness at the same level as the base metal (Fig. 8, b). However, the martensitic structure (Fig. 7, d) with increased microhardness (Fig. 8, c), as well as microcracks along the weld (Fig. 6, c) are also formed when the amount of heat input exceeds the optimum values by increasing frequency (modes 8, 9 and 10). As a consequence, after the strength test the specimens have been failed in a ductile-brittle manner (Fig. 9, a), in contrast to the base metal which has a classic ductile fracture appearance (Fig. 9, b).

The branched surface microcracks which can be visible only using a microscope were also revealed on all welds. The most typical example is shown in Fig. 6, e. These cracks are difficult to classify according to the cause of their occurrence due to the fact that they were not found during visual inspection, but the period between welding and surface investigations using the microscope was several days. Both cold and hot cracks are very likely to form in laser welded joints, although the main causes of these imperfections differ [15–18]. The main cause of hot crack propagation is the combination of very fast elasto-plastic deformations and low plasticity of the welded metal when cooling in the brittle temperature range. In investigated cases, the low plasticity of the weld metal may be caused by contamination with gases from atmosphere and/or by the presence of the martensitic structure. The reasons for the formation of cold cracks are high residual stresses and high content of hydrogen in the metal. This is also one of the basic problems of zirconium alloys according to [5,6,46]. However, the available EDS analyzer does not allow determining the amount

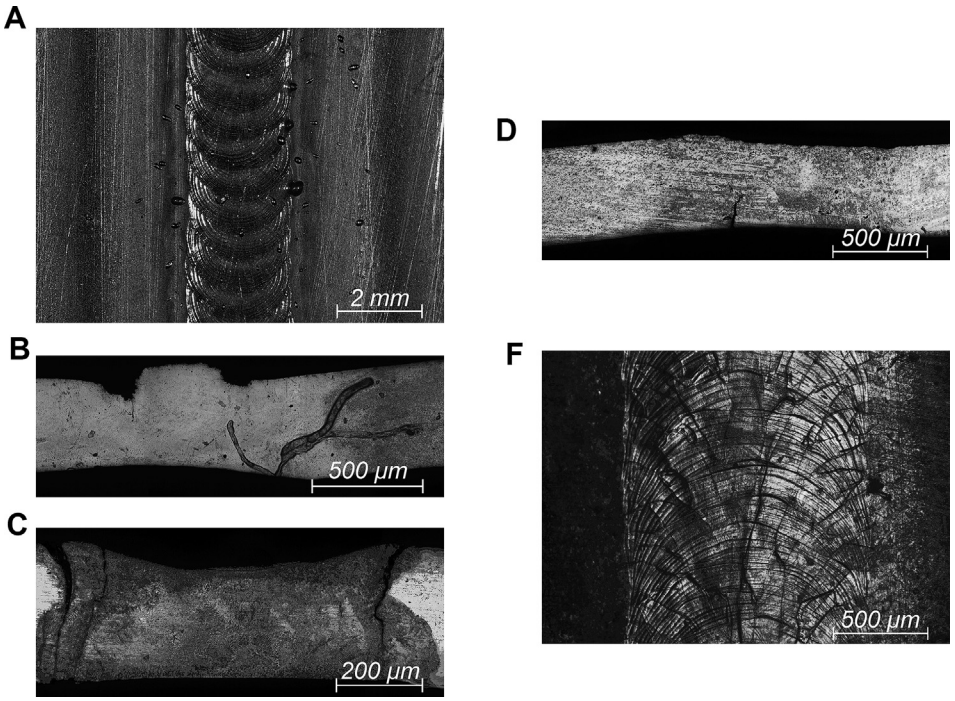

Fig. 6. Typical imperfections of welded joints: a – discoloration and spatter (mode 4), b – local intermittent undercuts, gas pores and cavities (mode 8), c and d – longitudinal microcracks (modes 1 and 10), e – branching microcracks (mode 9).

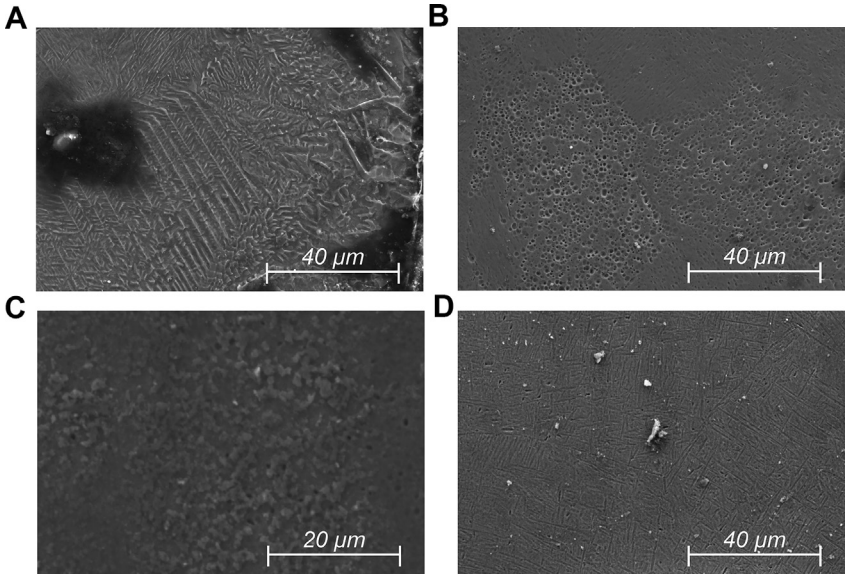

Fig. 7. Microstructure of weld metal: a – mode 1, b – mode 2, c – mode 6, d – mode 10.

of hydrogen in the metal. In this regard, more research is needed using the specialized equipment.

4. Conclusion

Based on the results of the research, the following conclusions can be drawn:

1. The most efficient combination of parameters for pulsed laser welding of Zr–1%Nb sheets with a thickness of 0.5 mm (butt joints) among the investigated is as follows: 8–11 J pulse energy, 10–14 ms pulse duration, 780–810 W peak pulse power, 3 Hz pulse frequency, 1.12 mm/s welding speed. The overlapping factor is 61% with these parameters and the laser beam with a diameter of 0.95 mm.
2. The obtained results show that ultimate strength under static loading can not be used as a quality criterion for zirconium alloys welds.
3. Increased shielding gas flow rate does not allow to protect weld metal totally and contributes to defects formation without using special nozzles.

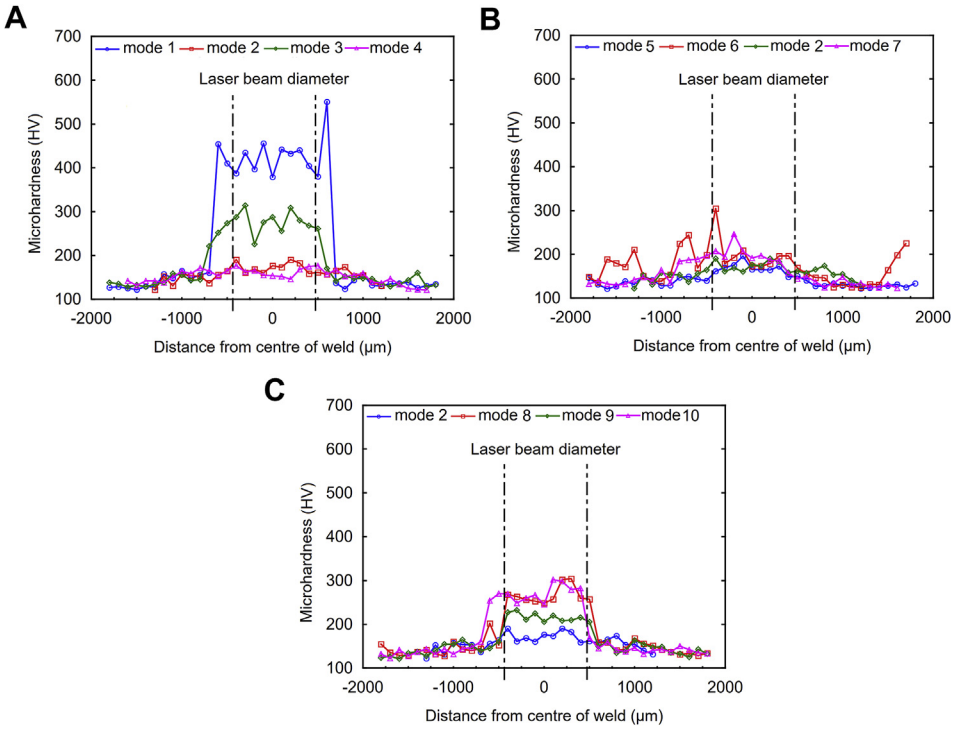

Fig. 8. Microhardness of weld metal: a – modes 1, 2, 3 and 4, b – modes 2, 5, 6 and 7, c –modes 2, 8, 9 and 10.

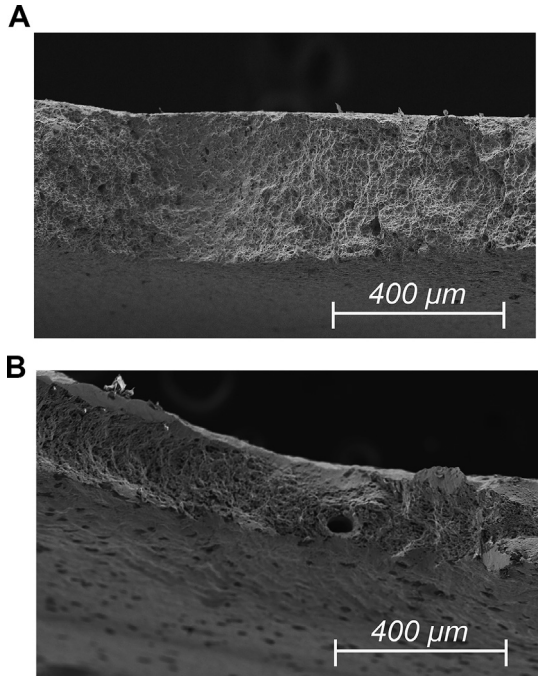

Fig. 9. Fractography of fracture surfaces: a – welds failure in a ductile-brittle manner, b – base metal failure in a ductile manner.

4. The major problem was branching microcracks on the surface of the welds but additional studies are required to determine the cause of their occurrence. It is necessary to improve the welding zone protection (gas composition and flow rate as well as nozzle configuration) and to study the hydrogen content in the welds.

Conflicts of interest

None.

References

[1] P. Rudling, R. Adamson, B. Cox, F. Garzarolli, A. Strasser, High burnup fuel issues, Nuclear Engineering and Technology 40 (1) (2008) 1–8.
[2] Quality and Reliability Aspects in Nuclear Power Reactor Fuel Engineering, International Atomic Energy Agency, Vienna, 2015.
[3] A.V. Nikulina, A.G. Malgin, Impurities and their effect on the structure and properties of zirconium parts in nuclear reactors, Atom. Energy 105 (5) (2008) 328–339.
[4] Russian Technical Specification TU 95.166-98 Zirconium Alloys in Ingots (In Russian).
[5] S.A. Nikulin, Zirconium Alloys for Nuclear Power Reactors, MISiS, Miscow, 2007 (In Russian).
[6] Physical material science, in: B.A. Kalin (Ed.), Part 1: Structural Materials for Nuclear Engineering, vol. 6, MEPhI, Moscow, 2008 (In Russian).
[7] ISO 9606-5:2000 Approval Testing of Welders – Fusion Welding – Part 5: Titanium and Titanium Alloys, Zirconium and Zirconium Alloys.
[8] ISO 15614-5:2004 Specification and Qualification of Welding Procedures for Metallic Materials – Welding Procedure Test – Part 5: Arc Welding of Titanium, Zirconium and Their Alloys.
[9] AWS G2.5/G2.5M:2012 Guide for the Fusion Welding of Zirconium and Zirconium Alloys.
[10] Russian Technical Specification OST 95 503-2006 Welded and Brazed Joints of Parts of Nuclear Reactor Cores. General Technical Requirements. Acceptance Rules and Quality Control Methods (In Russian).
[11] Russian Technical Specification OST 95 877-2011 Nuclear Reactors. Nuclear Reactor Cores. Welded and Brazed Joints. Design and Organization of Manufacturing Processes Rules (In Russian).
[12] Review of Fuel Failures in Water Cooled Reactors, International Atomic Energy Agency, Vienna, 2010.
[13] P. Mishra, V.P. Jathar, J.L. Singh, D.N. Sah, P.K. Shah, S. Anantharaman, In-reactor degradation of fuel and cladding in fuel pins operated with weld defects, J. Nucl. Mater. 439 (1–3) (2013) 217–223.
[14] M.S. Slobodyan, Methods of creation of permanent zirconium alloy joints in reactor art: a review, Tsvetnye Met. 10 (2016) 91–98.
[15] A.G. Grigoriyants, Fundamentals of Laser Processing of Materials, Mechanical engineering, Moscow, 1989 (In Russian).
[16] S. Katayama (Ed.), Handbook of Laser Welding Technologies, Woodhead Publishing Limited, Cambridge, 2013.
[17] D. Havrilla, Process Fundamentals of Industrial Laser Welding and Cutting,

Rofin-Sinar Inc., Plymouth, 1999.
[18] C. Dawes, Laser Welding: a Practical Guide, Woodhead Publishing Limited, Cambridge, 2008.
[19] X.-L. Gao, J. Liu, L.-J. Zhang, J.-X. Zhang, Effect of the overlapping factor on the microstructure and mechanical properties of pulsed Nd:YAG laser welded Ti6Al4V sheets, Mater. Char. 93 (2014) 136–149.
[20] R. Johnson, Lasers in the nuclear industry, in: Laser Weld, Cutting and Surface Treatment, The Welding Institute, Abington, 1984, pp. 43–47.
[21] V. Ram, G. Kohn, A. Stern, CO_2 laser beam weldability of Zircaloy-2, Weld. J. 65 (7) (1986) 33–38.
[22] F.G. Reshetnikov (Ed.), Development, Production and Operation of Fuel Rods of Power Reactors, vol. 2, Energoatomizdat, Moscow, 1995 (In Russian).
[23] S.-S. Kim, C.-Y. Lee, M.S. Yang, Investigation on Nd:YAG laser weldability of Zircaloy-4 end cap closure for nuclear fuel elements, Journal of the Korean Nuclear Society 33 (2) (2001) 175–183.
[24] Q. Wan, X. Bai, X. Liu, Impact of yttrium ion implantation on corrosion behavior of laser beam welded Zircaloy-4 in sulfuric acid solution, Appl. Surf. Sci. 252 (5) (2005) 1974–1980.
[25] Q. Wan, X. Bai, X. Zhang, Impact of high dose krypton ion irradiation on corrosion behavior of laser beam welded Zircaloy-4, Mater. Res. Bull. 41 (2) (2006) 387–395.
[26] K. Une, S. Ishimoto, Crystallographic measurement of the β to α phase transformation and δ-hydride precipitation in a laser-welded Zircaloy-2 tube by electron backscattering diffraction, J. Nucl. Mater. 389 (2009) 436–442.
[27] K.-N. Song, S.-S. Kim, S.-H. Lee, S.-B. Lee, Laser welding unit for intersection line welding of spacer grid inner straps and its application, Journal of Laser Micro/Nanoengineering 4 (1) (2009) 11–17.
[28] K.-N. Song, S.-D. Hong, S.-H. Lee, H.-Y. Park, Effect of mechanical properties in the weld zone on the structural analysis results of a plate-type heat exchanger prototype and pressurized water reactor spacer grid, J. Nucl. Sci. Technol. 49 (9) (2012) 947–960.
[29] K.-N. Song, S.-H. Lee, Effect of weld properties on the crush strength of the PWR spacer grid, Science and Technology of Nuclear Installations 2012 (2012) 540285, https://doi.org/10.1155/2012/540285.
[30] N. Boutarek, B. Azzougui, D. Saidi, M. Neggache, Microstructure change in the interface of CO_2 laser welded zirconium alloys, Physics Procedia 2 (3) (2009) 1159–1165.
[31] D.H. Jeong, J.H. Kim, Fatigue characteristics of laser welded Zircaloy thin sheet, Int. J. Mod. Phys.: Conference Series 6 (2012) 367–372.
[32] Q. Han, D. Kim, D. Kim, H. Lee, N. Kim, Laser pulsed welding in thin sheets of Zircaloy-4, J. Mater. Process. Technol. 212 (2012) 1116–1122.
[33] W. Tao, C. Cai, L. Li, Y. Chen, I.L. Wang, Pulsed laser spot welding of intersection points for Zircaloy-4 spacer grid assembly, Mater. Des. 52 (2013) 487–494.
[34] S. Livingstone, L. Xiao, E.C. Corcoran, G.A. Ferrier, K.N. Potter, Development of laser welded appendages to Zircaloy-4 fuel tubing (sheath/cladding), Nucl. Eng. Des. 284 (2015) 97–105.
[35] S. Kim, W. Lee, D. Kim, One-step distortion simulation of pulsed laser welding with multi-physics information, Int. J. Simulat. Model. 14 (1) (2015) 85–97.
[36] S. Kim, W.-J. Lee, Q. Han, D. Kim, Pulsed laser induced mechanical behavior of Zircaloy-4, J. Mater. Res. 30 (4) (2015) 556–565.
[37] C. Cai, W. Tao, L. Li, Y. Chen, Weld bead formation and corrosion behavior of pulsed laser welded zirconium alloy, Int. J. Adv. Manuf. Technol. 77 (2015) 621–628.
[38] C. Cai, L. Li, W. Tao, G. Peng, X. Wang, Weld bead size, microstructure and corrosion behavior of zirconium alloys joints welded by pulsed laser spot welding, J. Mater. Eng. Perform. 25 (2016) 3783–3792.
[39] S.-S. Kim, G.-I. Park, J.-H. Koh, Laser welding of dissimilar sheath metals, Mater. Sci. Forum 580–582 (2008) 493–499.
[40] H. Serizawa, Y. Asakura, H. Motoki, D. Tanigawa, M. Tsukamoto, J.-S. Park, H. Kishimoto, A. Kohyama, Development of joining method between Zircaloy and SiC/SiC composite tubes by using diode laser, Mater. Sci. Forum 879 (2017) 1743–1748.
[41] J.-N. Yang, L.-J. Zhang, J. Ning, Q.-L. Bai, J.-Y. Pei, J.-Z. Liu, G.-F. Lu, J.-X. Zhang, Fiber laser welding characteristics of commercially pure zirconium (R60702) and structure-mechanics-corrosion performances of the joint, Int. J. Refract. Metals Hard Mater. 73 (2018) 58–73.
[42] S.S. Mahlalela, P.G.H. Pistorius, Microstructural characterization of laser beam and gas tungsten arc welded zirconium-2.5Nb, J. S. Afr. Inst. Min. Metall 117 (10) (2017) 947–953.
[43] J. Chen, A. Khalifa, L. Xue, M. King, Laser weldability of Zr-2.5Nb alloy to AISI 410 stainless steel with Ni filler, J. Mater. Process. Technol. 255 (2018) 184–194.
[44] G. Satyanarayana, K.L. Narayana, B. Nageswara Rao, Numerical simulations on the laser spot welding of zirconium alloy endplate for nuclear fuel bundle assembly, Lasers in Manufacturing and Materials Processing 5 (1) (2018) 53–70.
[45] G. Satyanarayana, K.L. Narayana, B. Nageswara Rao, Identification of optimum laser beam welding process parameters for E110 zirconium alloy butt joint based on Taguchi-CFD simulations, Lasers in Manufacturing and Materials Processing 182 (5) (2018), https://doi.org/10.1007/s40516-018-0061-7.
[46] A.S. Zaymovskiy, A.V. Nikulina, N.G. Reshetnikov, Zirconium Alloys in Nuclear Energy, Energoizdat, Moscow, 1994 (In Russian).
[47] ANSI/AWS B4.0-2007 Standard Methods for Mechanical Testing of Welds.
[48] ISO 6507-1:2018 Metallic Materials – Vickers Hardness Test – Part 1: Test Method.
[49] ISO 22826:2005 Destructive Tests on Welds in Metallic Materials – Hardness Testing of Narrow Joints Welded by Laser and Electron Beam (Vickers and Knoop Hardness Tests).
[50] ISO 6520-1:2007 Welding and Allied Processes – Classification of Geometric Imperfections in Metallic Materials – Part 1: Fusion Welding.